Polymer 55 (2014) 1040–1047

Contents lists available at ScienceDirect

Polymer

journal homepage: www.elsevier.com/locate/polymer

Effect of polymer structure on the molecular dynamics and thermal behavior of poly(allyl acetoacetate) and copolymers

Katarzyna Grzybowska [a,*], Zaneta Wojnarowska [a], Andrzej Grzybowski [a], Marian Paluch [a], Juan M. Giussi [b], M. Susana Cortizo [b], Iwona Blaszczyk-Lezak [c], Carmen Mijangos [c]

[a] Institute of Physics, University of Silesia, ul. Uniwersytecka 4, 40-007 Katowice, Poland
[b] Laboratorio de Estudio de Compuestos Orgánicos (LADECOR), Instituto de Investigaciones Fisicoquímicas Teóricas y Aplicadas (INIFTA), CONICET CCT-La Plata, Facultad de Ciencias Exactas, UNLP (1900), 47 y 115 La Plata, Argentina
[c] Instituto de Ciencia y Tecnología de Polímeros, CSIC, Juan de la Cierva 3, 28006 Madrid, Spain

ARTICLE INFO

Article history:
Received 9 September 2013
Received in revised form
12 December 2013
Accepted 6 January 2014
Available online 12 January 2014

Keywords:
Copolymers
Molecular dynamics
Glass transition

ABSTRACT

In this paper, dielectric and calorimetric studies of the small-molecule glass former allyl acetoacetate monomers as well as its newly synthetized homopolymer and copolymers with different styrene composition were performed in both the liquid and glassy states. The molecular dynamics studies by the broadband dielectric spectroscopy and the stochastic temperature modulated differential scanning calorimetry enabled us to explore relaxation processes of examined materials in the wide frequency range. We found that the copolymers reveal two co-existing glass transitions characterized by the glass transition temperatures, which are very close to those of the corresponding homopolymers. These results suggest that the copolymers exhibited some sequences of acetoacetate units with a microphase-separated morphology in agreement with the value of reactivity ratio previously determined. We investigated effects of copolymerization compositions on the glass transition temperature, the isobaric fragility index, the dielectric and calorimetric intensity, and the dynamic heterogeneity on the glass transitions of the materials.

1. Introduction

Synthetic polymers containing tautomeric functional groups have emerged as important materials due to their potential applications. The presence of tautomeric units on the main polymer chain was used to immobilize different ion. In particular, allyl acetate is a very interesting organic compound to complex many transition metal ions. The interest of this group as ligand has increased recently due to unique magnetic or catalytic properties of the complex particles [1]. Papaphilippou et al., studied a series of copolymers including 2-(acetoacetoxy)ethyl methacrylate metal-chelating monomer, in which β-ketoester functionalities act as effective stabilizers for iron oxide nanoparticles in aqueous solutions [2]. Subsequently, Pd nanoparticles encapsulated in AEMA-containing diblock copolymer micelles were synthesized and investigated towards nonlinear optical (NLO) properties [3]. The most studied tautomeric monomers are β-dicarbonyl derivatives, mainly due to the ease of synthesis and prior knowledge of structurally related compounds of low molecular weight [4,5]. Among β-dicarbonyl monomers, allyl acetate has been extensively studied by Bartlett and Altschul in a radical polymerization process [6]. In this reaction, a competition between the fundamental reactions of addition to the double bond (polymerization) and hydrogen abstraction (chain transfer) can be observed [7]. Recently, we have synthesized and characterized two kinds of tautomeric acetoacetate copolymers with different compositions, structure and properties [8].

Besides the chemical characterization of the newly synthesized copolymers it is very important to investigate their thermal behavior and molecular dynamics under different conditions. Determining the molecular mobility of copolymers enables us to gain a better insight into properties of copolymers, in particular dynamics of the glass transition, which are strongly dependent on the composition, architecture, and morphology of the copolymers. Such investigations can consequently lead to an improvement of the polymeric materials. A very useful method for establishing molecular mobility of polymers is the broadband dielectric spectroscopy (BDS), which enables measurements of relaxation times over a wide frequency range up to 12 decades at different temperatures. The BDS study can be combined with the temperature modulated differential scanning calorimetry (TMDSC) measurements, which usually cover only a narrow frequency range near the

* Corresponding author.
E-mail address: katarzyna.grzybowska@us.edu.pl (K. Grzybowska).

0032-3861/$ – see front matter © 2014 Elsevier Ltd. All rights reserved.
http://dx.doi.org/10.1016/j.polymer.2014.01.006

glass transition, but can facilitate the identification of the origin of relaxation processes observed in the dielectric and mechanical spectra [9]. Homopolymers and more complex systems like copolymers usually exhibit several relaxation processes of different nature in the dielectric relaxation spectra. In polymers, the main relaxation process (α-relaxation) associated with the glass transition temperature is related to segmental dynamics of the chain. Besides the linear-chain polymers, dielectric analysis has been applied to numerous macromolecular systems with complex molecular architectures, namely, comblike and branched structures, stars, cycles, copolymers (alternate, statistical, di or multiblock copolymers), physically or chemically bonded polymer networks, hyperbranched polymers, and dendrimers. The molecular dynamics of such systems involves a series of relaxation processes that goes from very local motions (generally due to branching chains or side-chains) to segmental mobility exhibiting cooperativity (α relaxation), or even large-scale relaxation processes (Rouse dynamics or reptation) [10,11]. For instance, some block copolymers have complex phase diagram that may show microphase separation [12,13] and they can reveal more than one segmental relaxation associated with the glass transition of each block [14–21]. The temperature behavior of structural relaxation times of each block is usually similar to that of the corresponding homopolymer [22]. However, the shape of the structural relaxation is much broader in copolymers than that in homopolymers, which is often related to an increase in the dynamic heterogeneity or cooperativity of segmental motions in copolymers [15,22]. These investigations have been considerably enriched by high pressure measurements [23], enabling for instance an additional verification of ideas that originally assumed ambient pressure conditions. Besides segmental dynamics the secondary relaxations can be also observed in dielectric spectra of polymers. The secondary processes usually reflect some fluctuations of parts of the polymer mainchain, conformational changes in cyclic side groups, or hindered rotations of side groups or parts of them [10,11,24–27]. This type of local dynamics remains active even when the polymer is in the glassy state, that is, when the large lengthscale backbone motions are frozen.

In this paper, we report results of a comparative analysis of allyl acetoacetate (AAA) monomer, its homopolymer and two copolymers with styrene (St-co-AAA) of different mole fraction of monomer AAA, i.e. $F_{AAA} = 0.45$ (St-co-AAA1) and $F_{AAA} = 0.17$ (St-co-AAA2). We focus on molecular dynamics studies of the materials in the wide temperature range in both the liquid and glassy states by using the broadband dielectric spectroscopy and stochastic temperature modulated differential scanning calorimetry. We investigate the effect of the polymer structure on the molecular dynamics and thermal behavior properties of PAAA and poly(St-co-AAA).

2. Experimental section

2.1. Materials

Allyl acetoacetate monomer (AAA, 98%, Aldrich) was used as received. The initiator, 2,2′-azobis-(isobutyronitrile) (AIBN, 98%, Merck) was purified by recrystallization from methanol before use. Methanol (99.9%, Aldrich), chloroform (RPE, Carlo Erba), acetonitrile (HPLC, Sintorgan), tetrahydrofuran (RPE, Carlo Erba), sodium bicarbonate (99.5%, Fluka), and anhydrous sodium sulfate (99%, Anedra) were used as received without further purification. Styrene (>99%, Aldrich) was freed from inhibitor by washing with aqueous NaOH solution (10 wt%) and then with water until neutrality, dried over anhydrous sodium sulfate, and distilled under reduced pressure before use.

Polymerization: PAAA homopolymer and two poly(St-co-AAA) copolymers were synthesized by mass radical polymerization with azobisisobutyronitrile as a radical initiator, as described by Giussi et al. in a previous paper [8]. Briefly, different amounts of both comonomers (total weight 10 ml) were introduced into a reaction tube with a pre-weighed amount of initiator (35 mM). The mixtures were degassed by three freeze–pump–thaw cycles in a vacuum line system, then sealed and immersed into a thermostat at 333 K at different times in the absence of light. After the reaction, polymers were precipitated with methanol and purified by three steps of dissolutions in chloroform and precipitation in methanol, centrifuged and dried under vacuum. This procedure was repeated until only the peak of the polymer was seen by size-exclusion chromatography (SEC). The chemical structure of the obtained copolymer is shown in Fig. 1.

Two copolymers poly(St-co-AAA)1 and poly(St-co-AAA)2 with different monomer composition were synthesized, starting at the same initial monomer feed, $f_{AAA} = 0.80$, at 4 and 16 h, respectively.

Characterization: The ^{1}H NMR and ^{13}C NMR spectra of the samples were recorded with a Bruker Spectrometer, 300 MHz. Chloroform-d1 was used as a solvent for the polymer. The sample concentrations were 0.4 and 6.0 wt% for monomer and polymer respectively. The measurements were carried out at 313 K.

The copolymers obtained were identified by NMR. ^{1}H NMR (300 MHz, chloroform-d_1, ppm) δ: 1.49 (>CH–C$\underline{H}_2$– St and AAA); 1.95 (>C$\underline{H}$–CH$_2$– St and AAA); 2.13 (C$\underline{H}_3$–C(O)– keto and C$\underline{H}_3$–C(OH)=enol AAA); 3.53 (–C(O)–C$\underline{H}_2$–C(O)– AAA); 4.13 (–C$\underline{H}_2$–O–C(O)– AAA); 5.06 (–C(OH)=C$\underline{H}$–C=O– enol AAA); 6.5–7.5 (ArH St). ^{13}C NMR (300 MHz, Chloroform-d_1, ppm) δ: 21.15 (–$\underline{C}$H$_3$ enol); 30.23 (–$\underline{C}$H$_3$ keto); 32.50 (>CH–$\underline{C}$H$_2$– AAA); 40.55 (>$\underline{C}$H–CH$_2$– AAA); 42.78 (>$\underline{C}$H–CH$_2$– St); 44.06 (>$\underline{C}$H–CH$_2$– St); 49.92 (–C(O)–$\underline{C}$H$_2$–C(O)– keto); 68.02 (>CH–$\underline{C}$H$_2$–O–C(O)–); 89.75 (–C(O)–$\underline{C}$H=COH); 125.66 (ortho–$\underline{C}$ Ar); 127.72 (meta–$\underline{C}$ Ar); 128.02 (para–$\underline{C}$ Ar); 145.29 (ipso–$\underline{C}$ Ar); 166.88 (>$\underline{C}$=O ester); 175.31 (HO–$\underline{C}$= enol); 200.01 (>$\underline{C}$=O keto).

The copolymer compositions were estimated from the integral ratio of selected peaks of ^{1}H NMR, using the following formula [8]: $F_{AAA} = 5I_{CH_2}(h)/(5I_{CH_2}(h) + 2I_{Ar})$, where I_{CH_2} and I_{Ar}, are the intensity of the signals of allyl ($\delta = 4.13$ ppm) and aromatic hydrogen ($\delta = 6.5$–7.5 ppm), respectively.

The average molecular weight and the molecular weight distribution were determined by SEC in an LKB-2249 instrument at 298 K. A series of four μ-styragel columns (10^5, 10^4, 10^3, 100 Å pore size) were used with chloroform as an eluent. The polymer concentration was 4–5 mg/mL, and the flow rate was 0.5 mL/min. The polymer was analyzed using double detection as previously reported [28]. Mass chromatograms of the polymers were detected by a Shimadzu (SPD-10A) UV/VIS detector at 254 nm (for the phenyl group), while the carbonyl group was detected by infrared (IR) absorption at 5.75 μm with a Miram 1A spectrophotometer detector. Polystyrene standard supplied by Polymer Laboratories and Polysciences were used for calibration.

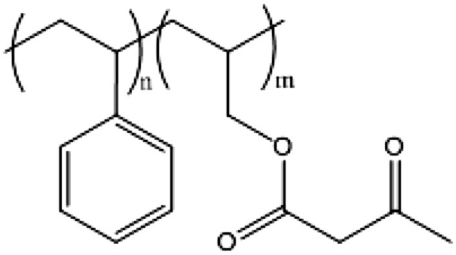

Fig. 1. Chemical structure of synthesized copolymers poly(St-co-AAA).

2.2. Broadband dielectric spectroscopy (BDS)

Isobaric measurements of the complex dielectric permittivity $\varepsilon^*(\omega) = \varepsilon'(\omega) - i\varepsilon''(\omega)$ were carried out using the Novo-Control Alpha dielectric spectrometer over frequency range from $3\cdot10^{-1}$ to 10^7 Hz at ambient pressure in the temperature range 133–403 K. The temperature stability controlled by Quatro System using a nitrogen gas cryostat was better than 0.1 K. Dielectric measurements of allyl acetoacetate (AAA) monomer, its homopolymer (PAAA) and copolymers with styrene (St-co-AAA1 and St-co-AAA2) were performed in a parallel-plate cell (diameter: 20 mm, gap: 0.1 mm) after 40 min drying in nitrogen atmosphere at 393 K.

2.3. Differential scanning calorimetry (DSC)

Calorimetric measurements of (AAA) monomer, PAAA homopolymer and copolymers with styrene (St-co-AAA1 and St-co-AAA2) were carried out by Mettler-Toledo DSC apparatus equipped with a liquid nitrogen cooling accessory and a HSS8 ceramic sensor (heat flux sensor with 120 thermocouples). Temperature and enthalpy calibrations were performed by using indium and zinc standards. Aluminum pans (40 μL) with samples have been top sealed with one puncture. Calorimetric measurements of each material were performed after its about 40 min drying in nitrogen atmosphere at 393 K or 403 K. Standard DSC measurements were performed at the heating rate of 10 K/min under nitrogen atmosphere (60 ml/min) in the wide temperature range 213–393 K (in the case of polymeric materials) and 143–363 K in the case of monomer AAA.

To obtain the accurate temperature dependences of heat capacity $C_p(T)$ and evaluate the structural relaxation times of investigated materials near the glass transition, a stochastic temperature-modulated differential scanning calorimetry (TMDSC) technique implemented by Mettler-Toledo TOPEM® has been exploited. In this experiment the sample was heated at rate of 0.5 K/min and temperature amplitude of the pulses of 0.5 K was selected. To achieve higher accuracy of the heat capacity we adjusted our evaluations using a sapphire reference curve. The calorimetric structural relaxation times $\tau_\alpha = 1/2\pi f$ have been determined from the temperature dependences of the real part of the complex heat capacity $C'_p(T)$ obtained at different frequencies in the glass transition region. The glass transition temperature T_g was determined for each frequency as the temperature of the half step height of $C'_p(T)$.

3. Results and discussion

3.1. Synthesis and characterization of polymers

In Table 1 the main characteristics of polymer and copolymers are summarized. The molecular weight M_w of homopolymer is 5900 g/mol and the polydispersity (PDI) is 2.2. The so low M_w obtained is expected since it is known that the AAA monomer is difficult to polymerize, yielding polymers of medium-molecular-weight or oligomers, due to the degradative monomer chain transfer [29].

Table 1
Characterization data for copolymers: reaction times, monomer mole fraction in the initial mixture of the monomers (f_{AAA}), monomer mole fraction in the polymers (F_{AAA}), weight-average molecular weights (M_w) and polydispersity index (PDI) of the copolymers synthesized.

Polymer	Time (h)	f_{AAA}	F_{AAA}	M_w (g/mol)	PDI
PAAA	16	1.00	1.00	5900	2.20
St-co-AAA1	4	0.80	0.45	20,820	1.97
St-co-AAA2	16	0.80	0.17	21,800	1.89

The molecular composition of the copolymers poly(St-co-AAA1) and poly(St-co-AAA2), obtained at 4 and 16 h is 0.45 and 0.17 respectively. It means that when the reaction time increases, the monomer mole fraction of AAA in the copolymer decreases, putting in evidence the lower reactivity of this monomer. In a separate work [8], we have determined the reactivity ratio for the system: $r_1(AAA) = 0.13 \pm 0.05$ and $r_2(St) = 6 \pm 2$, with $r_1 r_2 = 0.80$, which suggests that the system exhibits an ideal copolymerization behavior [8]. This result could indicate that the macromolecular chain also includes some large sequences of each monomer, the presence of which is also suggested by DSC and BDS measurements in the next sections. In order to analyze this supposition, SAXS measurements have been carried out (see Supporting information), however, no confirmation of two structural blocks in the macromolecular chain was obtained. This finding suggests that only sequences of the different comonomers could exist in the copolymer structure.

3.2. Calorimetric study of the materials

The standard (i.e. non-modulated) DSC measurements have been performed in the wide temperature range to detect any thermal effects occurred in investigated materials. Fig. 2 presents the thermograms obtained for monomer AAA, PAAA as well as for copolymers St-co-AAA1 and St-co-AAA2. As can be seen in the thermograms, there are sigmoidal changes in the temperature dependences of the heat flow for each material which are characteristics of the glass transition. The thermograms for monomer and homopolymer show only single glass transitions, whereas those for St-co-AAA1 and St-co-AAA2 suggest two glass transitions for each copolymer.

To verify that the sigmoidal changes in the heat flow are related to glass transitions, stochastic temperature modulated DSC measurements (TOPEM) have been performed for all materials. This method provides very useful possibilities of the accurate evaluation of the quasi-static heat capacity ($C_{p0} = C^*_p(f\to0)$, where C^*_p is the frequency dependent complex heat capacity) as well as the simultaneous determination of the frequency dependence of the heat capacity over a small frequency range in a single measurement. The latter functionality enables us to check whether a thermal effect is frequency dependent as it is in the case of the glass transition.

Results of the TOPEM analysis are presented in Fig. 3. As observed, the temperature dependences of the real part of the

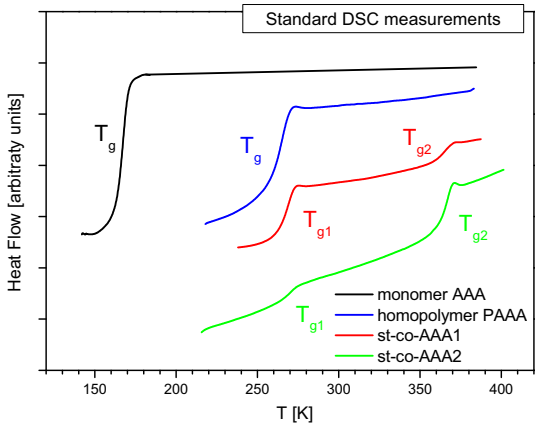

Fig. 2. DSC thermograms for AAA, PAAA and copolymers: St-co-AAA1 and St-co-AAA2 obtained at heating rate of 10 K/min.

quasi-static heat capacity C_{p0}, show single sigmoidal changes for monomer and homopolymer and two sigmoidal changes for each copolymer, similarly to those found in the temperature dependences of the heat flow measured by the standard DSC technique. Moreover, as can be seen in the insets in Fig. 3, we established that the temperature dependences of the real part of the complex heat capacity $C'_p(T)$ are frequency dependent within the temperature window of each sigmoidal change in the heat capacity for all investigated materials. It is also observed that the sigmoidal changes in the dependences $C'_p(T)$ shift towards high temperatures with increasing frequency. This behavior is characteristic of relaxation processes, for example, which occur during the vitrification process. As shown in the next section, the relaxation times determined from the frequency dependences of $C'_p(T)$ very well correspond to the structural relaxation times established from the dielectric spectroscopy experiment. This implies that the observed sigmoidal changes in $C'_p(T)$ are related to the glass transitions. The values of glass transition temperatures T_g (determined as the temperature of the half step height of the quasi-static heat capacity C_{p0}) and heat capacity steps ΔC_p at T_g for all examined materials are collected in Table 2.

Table 2
Glass transition parameters estimated from TOPEM analysis.

Material	$T_{g\ DSC}$ [K]	ΔC_p [J g^{-1} K^{-1}]	N_α
AAA	164.5	0.84	80
PAAA	263.0	0.47	123
St-co-AAA1	265.3 (low T_g)	0.37 (at low T_g)	89 (at low T_g)
Copolymer ($F_{AAA} = 0.45$)	362.3 (high T_g)	0.12 (at high T_g)	42 (at high T_g)
St-co-AAA2	267.0 (low T_g)	0.12 (at low T_g)	42 (at low T_g)
Copolymer ($F_{AAA} = 0.17$)	363.0 (high T_g)	0.22 (at high T_g)	145 (at high T_g)

It is worth noting that the value of $T_g = 263$ K for PAAA is considerably larger (of 98 K) than that for monomer AAA, whereas the lower value of the glass transition temperature for each copolymer is very close to T_g of PAAA and slightly increases with the decrease in the mole fraction of monomer AAA in copolymer

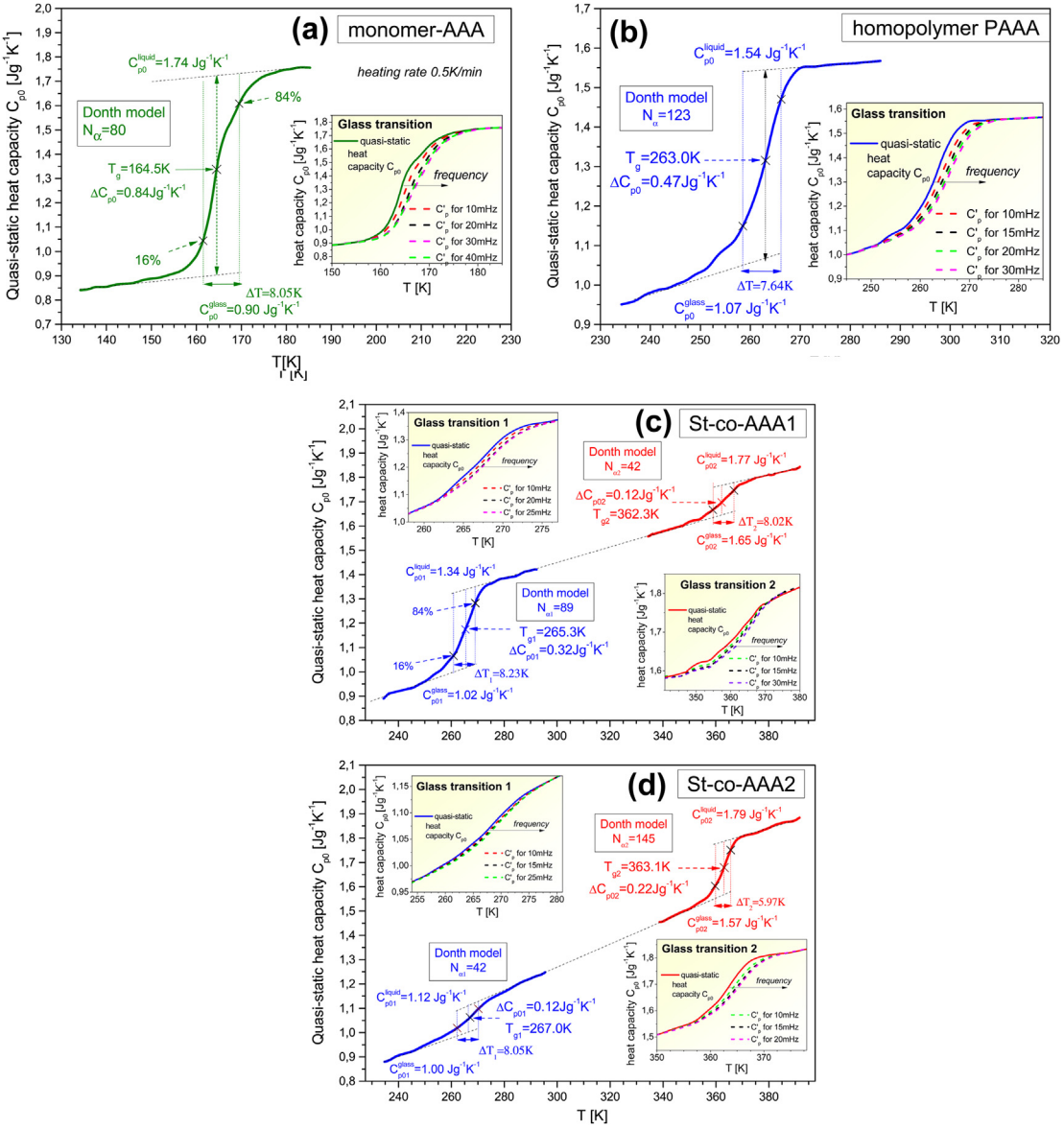

Fig. 3. Temperature dependences of quasi-static heat capacity C_{p0} (a) monomer AAA, (b) PAAA, (c) copolymer St-co-AAA1, and (d) copolymer St-co-AAA2. The insets show the temperature dependences of the real part of the complex heat capacity $C'_p(T)$ at selected frequencies for each glass transition.

($T_{g1} = 265.3$ K for St-co-AAA1 and $T_{g1} = 267$ K for St-co-AAA2). On the other hand, the value of $T_{g2} \approx 363$ K, which characterizes the second glass transition that occurs in copolymers at higher temperatures, well corresponds to the value of T_g of polystyrene (see Fig. 6 in Ref. [30]). This finding confirms that sequential units in copolymers are immiscible [18,31].

Another interesting observation is related to changes of the values of the heat capacity step ΔC_p at T_g due to polymerization and copolymerization. As can be seen in Fig. 3 and Table 2, the value of $\Delta C_p = 0.47$ J g^{-1} K^{-1} for PAAA homopolymer is considerably smaller than that for monomer AAA ($\Delta C_p = 0.84$ J g^{-1} K^{-1}) and larger than those for copolymers ($\Delta C_{p1} = 0.37$ J g^{-1} K^{-1} for St-co-AAA1 and $\Delta C_{p2} = 0.12$ J g^{-1} K^{-1} for St-co-AAA2) established at T_{g1} (their low glass transition temperature). The decrease in ΔC_p due to homopolymerization of AAA can be related to the decrease in the available configurations for the segmental motions in homopolymer during the glass transition in comparison with those for the monomer AAA motions reflected in its structural relaxation. The smaller values of ΔC_{p1} at T_{g1} for copolymers than that for PAAA can be also caused by a decrease in the available configurations for the segmental motions in the copolymers during their lower glass transition. However, it can result from a combined effect of copolymerization and mole fraction of monomer AAA in copolymers (because we found that ΔC_{p1} and ΔC_{p2} in copolymers decrease with decreasing mole fractions of monomers AAA and styrene, respectively).

A key factor that characterizes molecular dynamics of materials approaching the glass transition is the dynamic heterogeneity. This concept has been introduced by Adam and Gibbs who proposed the existence of molecular cooperatively rearranging regions (CRR), the size of which increases during vitrification process, consequently causing the dramatic increase in the time scale of molecular motions reflected in structural relaxation. The CRR can be interpreted as the smallest volume element that can relax to a new configuration independently of the neighboring regions. This point of view on the dynamic heterogeneity of molecular dynamics of copolymers, which is assumed herein, should be distinguished from the concept of the local heterogeneity considered by Lodge and McLeish [32] who focused on taking into consideration the chain connectivity in their model of local molecular dynamics of copolymers. Nevertheless, it should be noted that Schwartz et al. [33] incorporated the chain connectivity and the effect of pressure on the relaxation dynamics into the original Adam–Gibbs model to describe satisfactorily molecular dynamics of polymer blends. In this way, the Adam–Gibbs model has been shown to be a useful tool to investigate molecular dynamics of copolymers in ambient and elevated pressure conditions.

Based on the fluctuation theory, Donth proposed a formula to calculate the average number of particles (monomeric units in case of polymers [34,35] and copolymers [18]) N_α in CRR, and the characteristic length at the glass transition ξ_α (the characteristic size of CRR) from calorimetric data [36]

$$N_\alpha = \frac{\xi_\alpha^3 \rho N_A}{M} = \frac{RT_g^2 \Delta(1/C_V)}{M\delta T^2} \approx \frac{RT^2 \Delta(1/C_p)}{M\delta T^2} \quad (1)$$

where R is the gas constant, N_A is the Avogadro number, M is molecular weight of the relevant particle, $\Delta(1/C_p) = 1/C_p^{glass} - 1/C_p^{liquid}$ is calculated at T_g, and $\delta T = \Delta T/2.5$ is the temperature fluctuation obtained from the width ΔT of the glass transition, evaluated from the dependence $C_p(T)$ in the way depicted in detail in Fig. 3(a).

Analyzing the temperature dependences of C_{p0} by means of Donth method, we determined the average number of monomeric units N_α in CRR at each glass transition temperature of all investigated materials (see Fig. 3 and Table 2). We found that $N_\alpha = 123$ for PAAA, whereas $N_\alpha = 80$ for monomer AAA which indicates that the dynamic heterogeneity considerably increases due to the homopolymerization. On the other hand, the values of N_α evaluated for copolymers at their low glass transition temperature are significantly lower than that for PAAA, and decrease with decreasing mole fraction of monomer AAA in copolymers. Thus, we can conclude that the copolymerization decreases the dynamic heterogeneity. This finding is in agreement with the results reported by Encinar et al. [18] for a diblock copolymer (polystyrene-b-poly(t-butylacrylate)). The authors suggest that the smaller size of CRR for a given block relaxation in copolymer than that found for the segmental relaxation of the corresponding homopolymer can be due the microphase separated morphology of the diblock copolymer. In our copolymers, it could mean that the glassy phase of AAA sequences is constrained by the glassy phase of styrene sequences.

3.3. Dielectric study of the materials

The dielectric measurements have been performed for all obtained materials to investigate the effects of polymer structure on their molecular dynamics. Representative dielectric spectra for monomer AAA, PAAA, and copolymers: St-co-AAA1 and St-co-AAA2 obtained on heating the sample from the glassy to liquid state at atmospheric pressure are presented in Fig. 4.

To determine relaxation times of α and secondary processes at various temperatures for investigated materials we fitted the entire dielectric spectra using the following Havriliak–Negami (HN) formula supplemented with the dc conductivity contribution term [37]:

$$\varepsilon^*(\omega) = \varepsilon'(\omega) - i\varepsilon''(\omega) = \varepsilon_\infty + \sum_k \frac{\Delta\varepsilon_k}{\left[1 + (i\omega\tau_k)^{\xi_k}\right]^{\delta_k}} - i\frac{\sigma_0}{\varepsilon_0\omega}, \quad (2)$$

where ε_∞ is the high frequency limit permittivity and k stands for either the primary and the secondary processes, $\Delta\varepsilon_k$ is the relaxation strength, τ_k is the HN relaxation time, ξ_k and δ_k are the HN exponents of the relaxation processes, whereas σ_0 is the dc electrical conductivity and ε_0 is the dielectric permittivity of the vacuum.

From the best fits of dielectric spectra shown in Fig. 4 we found the temperature dependences of structural and secondary relaxation times for all examined materials (see Fig. 5). Additionally, we have determined the structural relaxation times $\tau_{\alpha DSC} = 1/2\pi f_{DSC}$ for each material from the temperature dependences of the real part of the complex heat capacity $C_p'(T)$ obtained at different frequencies f_{DSC} in the glass transition region presented in the insets in Fig. 3. The glass transition temperature T_g was determined for each frequency as the temperature of the half step height of $C_p'(T)$. As can be seen in Fig. 5, the obtained temperature dependences of calorimetric structural relaxation times $\tau_{\alpha DSC}$ very well corresponds to the temperature dependences of dielectric relaxation times. In this way, we can undoubtedly identify which dielectric relaxation is assigned to which glass transition detected in calorimetric measurements. As already mentioned, the identification is especially important in the case of copolymers characterized by the complex dielectric spectra.

To describe the temperature dependence of the dielectric structural α-relaxation times τ_α we used Vogel–Fulcher–Tammann (VFT) equation: [38–40]

$$\tau_\alpha(T) = \tau_\infty \exp\left(\frac{A}{T - T_0}\right) \quad (3)$$

where τ_∞, T_0, and A are fitting parameters. As can be seen in Fig. 5, the fitted VFT curves well describe the temperature dependences of

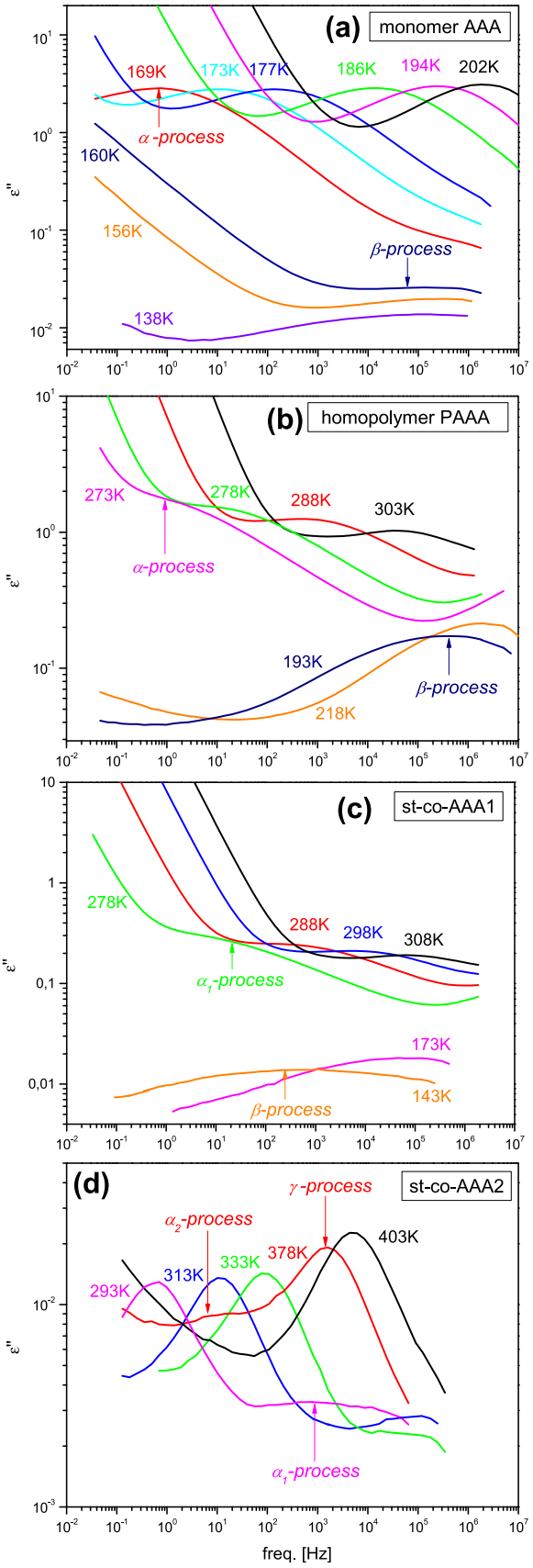

Fig. 4. Dielectric loss spectra of (a) AAA, (b) PAAA, (c) copolymer St-co-AAA1, and (d) copolymer St-co-AAA2 measured at different temperatures in both in the liquid and glassy states.

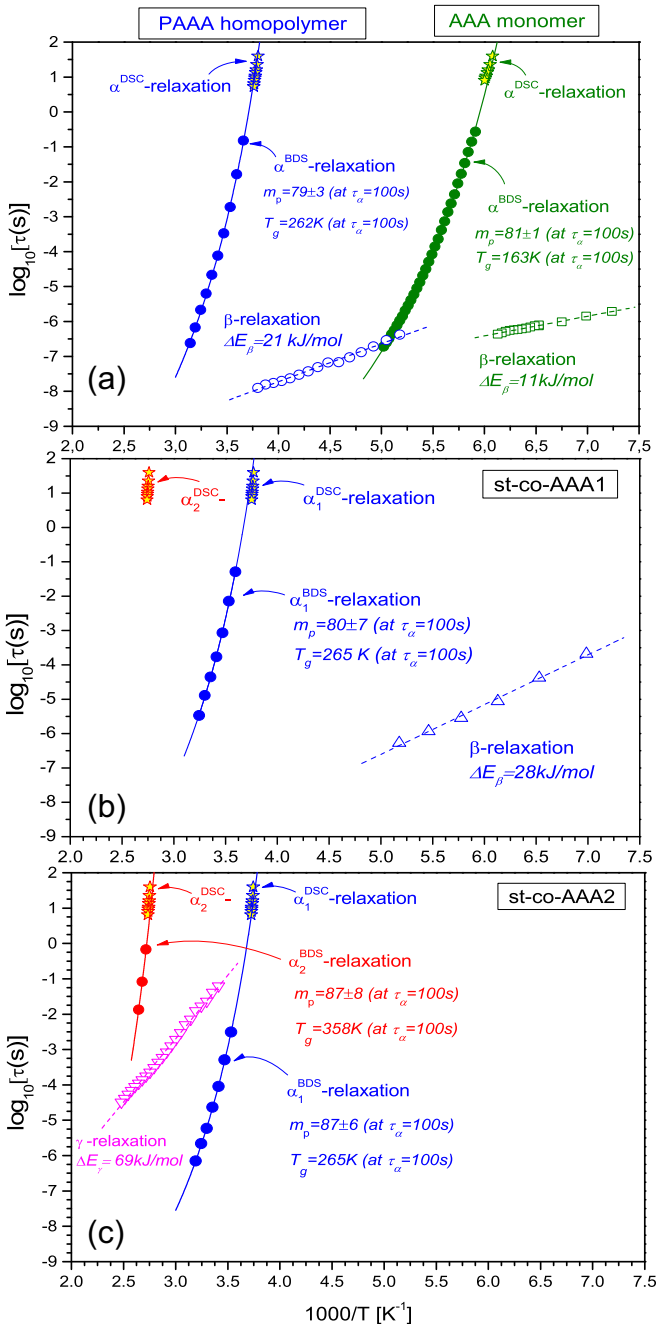

Fig. 5. Dielectric and calorimetric relaxation maps for (a) AAA monomer and PAAA, (b) copolymer St-co-AAA1, and (c) copolymer St-co-AAA2. Temperature dependences of dielectric structural relaxation times (α^{BDS}-relaxation, solid circles) were fitted to the VFT equation given by Eq. (3) (solid lines). The stars indicate the temperature dependences of the structural relaxation times (α^{DSC}-relaxation) determined from calorimetric TOPEM measurements. Temperature dependences of the dielectric secondary relaxations times (open points) were fitted to the Arrhenius equation given by Eq. (5) (dotted lines).

the dielectric structural relaxation times and their extrapolations to lower temperatures match the temperature dependences of the calorimetric relaxation times for each structural relaxation identified in studied materials.

From the fits of the dielectric $\tau_\alpha(T)$ dependences to the VFT equation we determined the dielectric glass transition temperatures of examined systems. Herein, we have applied the most frequently used definition, according to which T_g is the temperature at $\tau_\alpha = 100$ s. The dielectric glass transition temperatures found in

this way are in very good agreement with those obtained from calorimetric measurements (see Tables 2and 3).

One of important parameters that characterizes the structural relaxation is the fragility parameter, m_p defined as:

$$m_p \equiv \left.\frac{d\log \tau_\alpha}{d(T_g/T)}\right|_{T=T_g} \quad (4)$$

The values of m_p typically range between $m_p = 16$ and about 200 for various materials. The liquids characterized by small values of m_p are classified as *strong* systems, whereas large values of m_p are a feature of *fragile* materials. Molecular mobility in fragile liquids changes rapidly with temperature near T_g. Based on the values of the VFT parameters, we evaluated the values of m_p at $\tau_\alpha = 100$ s, which range from 79 to 87, however, we can assume that the values are the same taking into account uncertainties of their estimation (see Table 3). It should be noted that PAAA and polystyrene [41] characterized by similar values of m_p. Therefore, we can claim that neither polymerization nor copolymerization affect fragility of components of investigated polymers.

Now we consider the molecular mobility in the glassy state of the examined materials that is reflected in secondary relaxation processes. As already mentioned, each material exhibits a secondary relaxation process. The found temperature dependences of secondary relaxation times (see Fig. 5) obey the Arrhenius law (Eq. (5)).

$$\tau_\beta = \tau_\infty \exp\left(\frac{\Delta E_\beta}{RT}\right) \quad (5)$$

where the preexponential factor τ_∞ and the activation energy ΔE_β are the fitting parameters.

We found that the activation energy for the secondary relaxation of monomer AAA is very low ($\Delta E_\beta = 11$ kJ/mol). The low value of ΔE_β together with the symmetrical shape of β-peak suggests that some small angle local rotational motions of monomer AAA are responsible for this secondary relaxation.

The homopolymerization of monomer AAA results in an increase in ΔE_β, which is larger of 10 kJ/mol than that for monomer AAA, and the copolymerization leads to a further small increase in ΔE_β of 7 kJ/mol in the case of copolymer with the large content of AAA (St-co-AAA1). Similar and quite small values of ΔE_β for PAAA and copolymer St-co-AAA1 suggest that the secondary relaxations in these materials have the same molecular origin probably from localized rotational fluctuations of side chains.

The secondary relaxation γ observed in the dielectric spectra of the copolymer with the small content of AAA (St-co-AAA2) cannot rather origin from the styrene component, because the dielectric response of this material is much weaker [42] than that from the AAA component. One can suppose that some localized motions of the AAA monomers in a local environment rich in styrene monomers in the copolymer St-co-AAA2 are responsible for the secondary relaxation process γ, which is characterized by a considerably larger value of its activation energy $\Delta E_\gamma = 69$ kJ/mol than the value of ΔE_β in the copolymer St-co-AAA1. A similar secondary relaxation behavior has been previously reported for poly(styrene-co-methylmethacrylate) copolymers [43] and poly(-methyl methacrylate)/poly(ethylene oxide) blends [27].

Table 3
The glass transition temperatures T_g and the fragility parameters m_p determined from the dielectric structural relaxation.

Material	$T_{g\ BDS}$ [K] at $\tau_\alpha = 100$ s	m_p at $\tau_\alpha = 100$ s
AAA	163.3	81 ± 1
PAAA	262.0	79 ± 1
St-co-AAA1	265.3 (low T_g)	80 ± 3 (at low T_g)
Copolymer ($F_{AAA} = 0.45$)	– (High T_g)	– (At high T_g)
St-co-AAA2	265.0 (low T_g)	87 ± 6 (at low T_g)
Copolymer ($F_{AAA} = 0.17$)	258.0 (high T_g)	87 ± 8 (at high T_g)

4. Conclusions

In this paper, we investigated the thermal properties and molecular dynamics of the small-molecule glass former allyl acetoacetate as well as its newly synthetized homopolymer and copolymers with different contents of polystyrene. The dielectric and calorimetric measurements have been performed in both the liquid and glassy states of examined materials. We found that monomer AAA and homopolymer AAA are characterized by a single structural relaxation, and consequently by a single glass transition, whereas in each copolymer, we identified two separated glass transitions at the glass transition temperatures, which are very close to those of the corresponding homopolymers. The two coexisting glass transitions suggest that the copolymers exhibit sequences of acetoacetate units with a microphase-separated morphology.

Moreover, we found that the sizes of cooperative rearranging regions determined at T_g from the temperature dependences of C_p are smaller for the homopolymer AAA fraction in examined copolymers than that for the pure homopolymer AAA. It can result from a confinement of the glassy phase of AAA units in the glassy phase of styrene units.

The combined dielectric and calorimetric studies of molecular dynamics enabled us to explore relaxation processes in the wide frequency range. The relaxation maps obtained from dielectric and calorimetric measurements indicate that there are no differences in the temperature dependences of α-relaxations of homopolymer AAA and this compound built in the investigated copolymers. However, the dielectric strength of the α-process is considerably larger for homopolymer AAA than those for copolymers. We found the same pattern of behavior for ΔC_p. It suggests that the number of the available configurations for the segmental motions in the copolymers near the glass transition is smaller than that in the corresponding homopolymer.

The glassy states of the studied materials exhibit some molecular mobility reflected in the dielectric secondary relaxations. Similar and quite small values of the activation energies for secondary relaxations of homopolymer AAA and the copolymer rich in AAA segments (St-co-AAA1) suggest that the secondary processes in these materials originate from the same localized rotational fluctuations of side chains. On the other hand, the secondary relaxation observed in the copolymer rich in styrene segments (St-co-AAA2) can be attributed to some small localized motions of AAA monomers in a local environment rich in styrene monomers.

Acknowledgment

Authors are acknowledged to Dr Rebeca Hernandez for SAXS experiments. K.G., M.P., and Z.W. are grateful for the financial support from the Polish National Science Centre within the program OPUS3 (decision no. DEC-2012/05/B/ST3/02837). Z.W. acknowledges the financial assistance from FNP START (2013). I.B. and C.M. acknowledge MINECO for financial support (PRI PRIBAR 2011-1400 and MAT 2011–24797).

Appendix A. Supplementary data

Supplementary data related to this article can be found at http://dx.doi.org/10.1016/j.polymer.2014.01.006.

References

[1] Braddock DC, Chadwick D, Lindner-Lopez E. Tetrahedron Lett 2004;45:9021–4.
[2] Papaphilippou PC, Pourgouris A, Marinica O, Taculescu A, Athanasopoulos GI, Vekas L, et al. J Magn Magn Mater 2011;323:557.
[3] Iliopoulos K, Chatzikyriakos G, Demetriou M, Krasia-Christoforou T, Couris S. Opt Mater 2011;33:1342.
[4] Allegretti PE, Schiavoni MD, Guzman C, Ponzinibbio A, Furlong JJP. Eur J Mass Spectrom 2007;13:291–306.
[5] Novak P, Skare D, Sekusak S, Vikic-Topic D. Croat Chem Acta 2000;73:1153–70.
[6] Bartlett PD, Altschul R. J Am Chem Soc 1945;67:816–22.
[7] T Hill DJ, Odonnell HJ, Perera MCS, Pomery PJ. Eur Polym J 1997;33:1353–64.
[8] Giussi JM, Blaszczyk-Lezak I, Allegretti PE, Mijangos C, Cortizo MS. [Submitted].
[9] Wojnarowska Z, Wang Y, Pionteck J, Grzybowska K, Sokolov AP, Paluch M. Phys Rev Lett 2013;111:225703.
[10] Vassilikou-Dova A, Kalogeras IM. Chap. 6. In: Menczel Joseph D, Bruce Prime R, editors. Thermal analysis of polymers, fundamentals and applications. Wiley; 2009.
[11] Kremer F, Schönhals A. Broadband dielectric spectroscopy. Springer; 2003.
[12] Hamley IW. The physics of block copolymers. Oxford, UK: Oxford University Press; 1998.
[13] Morais V, Encinar Mario, Prolongo MG, Rubio RG. Polymer 2006;47:2349–56.
[14] Alig I, Floudas G, Avgeropoulos A, Hadjichristidis N. Macromolecules 1997;30:5004–11.
[15] Kyritsis A, Pissis P, Mai SM, Booth C. Macromolecules 2000;33:4581–95.
[16] Zhukov S, Geppert S, Stuhn B, Staneva R, Ivanova R, Gronski W. Macromolecules 2002;35:8521–30.
[17] Lorthioir C, Alegría A, Colmenero J, Deloche B. Macromolecules 2004;37:7808–17.
[18] Encinar M, Guzman E, Prolongo MG, Rubio RG, Sandoval C, Gonzalez-Nilo F, et al. Polymer 2008;49:5650–8.
[19] Mok MM, Masser KA, Runt J, Torkelson JM. Macromolecules 2010;43:5740–8.
[20] Sanz A, Nogales A, Ezquerra TA. Soft Matter 2011;7:6477–83.
[21] del Valle-Carrandi L, Alegría A, Arbe A, Colmenero J. Macromolecules 2012;45:491–502.
[22] Slimani MZ, Moreno AJ, Colmenero J. Macromolecules 2012;45:8841–52.
[23] Floudas G, Paluch M, Grzybowski A, Ngai K. Molecular dynamics of glass-forming systems: effects of pressure. Ch. 5. In: Kremer Friedrich, editor. Series: advances in dielectrics. Berlin, Heidelberg: Springer-Verlag; 2011.
[24] Mijovic J, Shen M, Wing Sy J, Mondragon I. Macromolecules 2000;33:5235–44.
[25] Jouenne S, Gonzalez-Leon JA, Ruzette AV, Lodefier P, Tencé-Girault S, Leibler L. Macromolecules 2007;40:2432–42.
[26] Yang J, Zheng X, Zhang B, Fu R, Chen X. Macromolecules 2011;44:1026–33.
[27] Jin X, Zhang S, Runt J. Macromolecules 2004;37:8110–5.
[28] Cortizo MS, Andreetta HA, Figini RV. High Resolut Chromatogr 1989;12:372–4.
[29] Matsumoto A, Kumagai T, Ota HA, Kawasaki H, Arakawa R. Polym J 2009;41:26–33.
[30] Schawe JEK, Hütter T, Heitz C, Alig I, Lellinger D. Thermochim Acta 2006;446:147–55.
[31] Buzin AI, Pyda M, Costanzo P, Matyjaszewski K, Wunderlich B. Polymer 2002;43:5563–9.
[32] Lodge TP, McLeish TCB. Macromolecules 2000;33:5278–84.
[33] Schwartz GA, Alegría Á, Colmenero J. J Chem Phys 2007;127:154907.
[34] Hempel E, Hempel G, Hensel A, Schick C, Donth E. J Phys Chem B 2000;104:2460–6.
[35] Huth H, Beiner M, Weyer S, Merzlyakov M, Schick C, Donth E. Thermochim Acta 2001;377:113–24.
[36] Donth E. J Non Cryst Solids 1982;53:325–30.
[37] Havriliak S, Negami S. J Polym Sci C 1966;14:99–117.
[38] Vogel HJ. Phys Z 1921;22:645–6.
[39] Fulcher GS. J Am Ceram Soc 1925;8:339–55.
[40] Tammann G, Hesse WZ. Anorg Allg Chem 1926;156:245–57.
[41] Huang D, Colucci DM, McKenna GB. J Chem Phys 2002;116:3925–34.
[42] Lupaşcu V, Picken SJ, Wübbenhorst M. J Non Cryst Solids 2006;352:5594–600.
[43] Encinar M, Prolongo MG, Rubio RG, Ortega F, Ahmadi A, Freire JJ. Eur Phys J E 2011;34:134.